

AD-A124 556

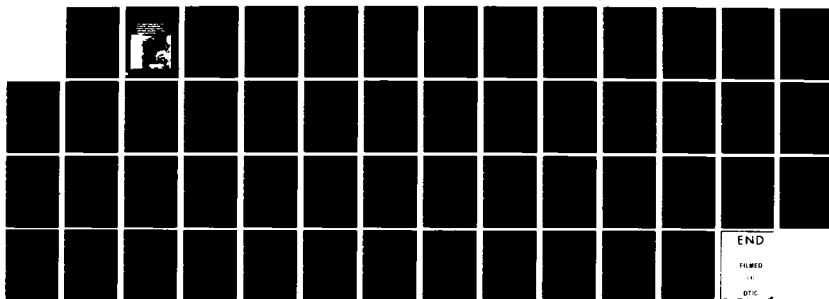
CHIP WAVEFORM SELECTION IN OFFSET-QUATERNARY
DIRECT-SEQUENCE SPREAD-SPECT. (U) ILLINOIS UNIV AT
URBANA COORDINATED SCIENCE LAB J S LEHNERT JAN 81
R-987 DAG29-78-G-0114

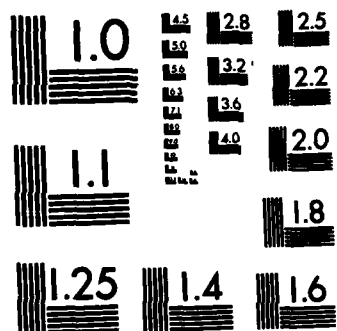
1/1

UNCLASSIFIED

F/G 17/2

NL





MICROCOPY RESOLUTION TEST CHART
NATIONAL BUREAU OF STANDARDS-1963-A

ADA 124556

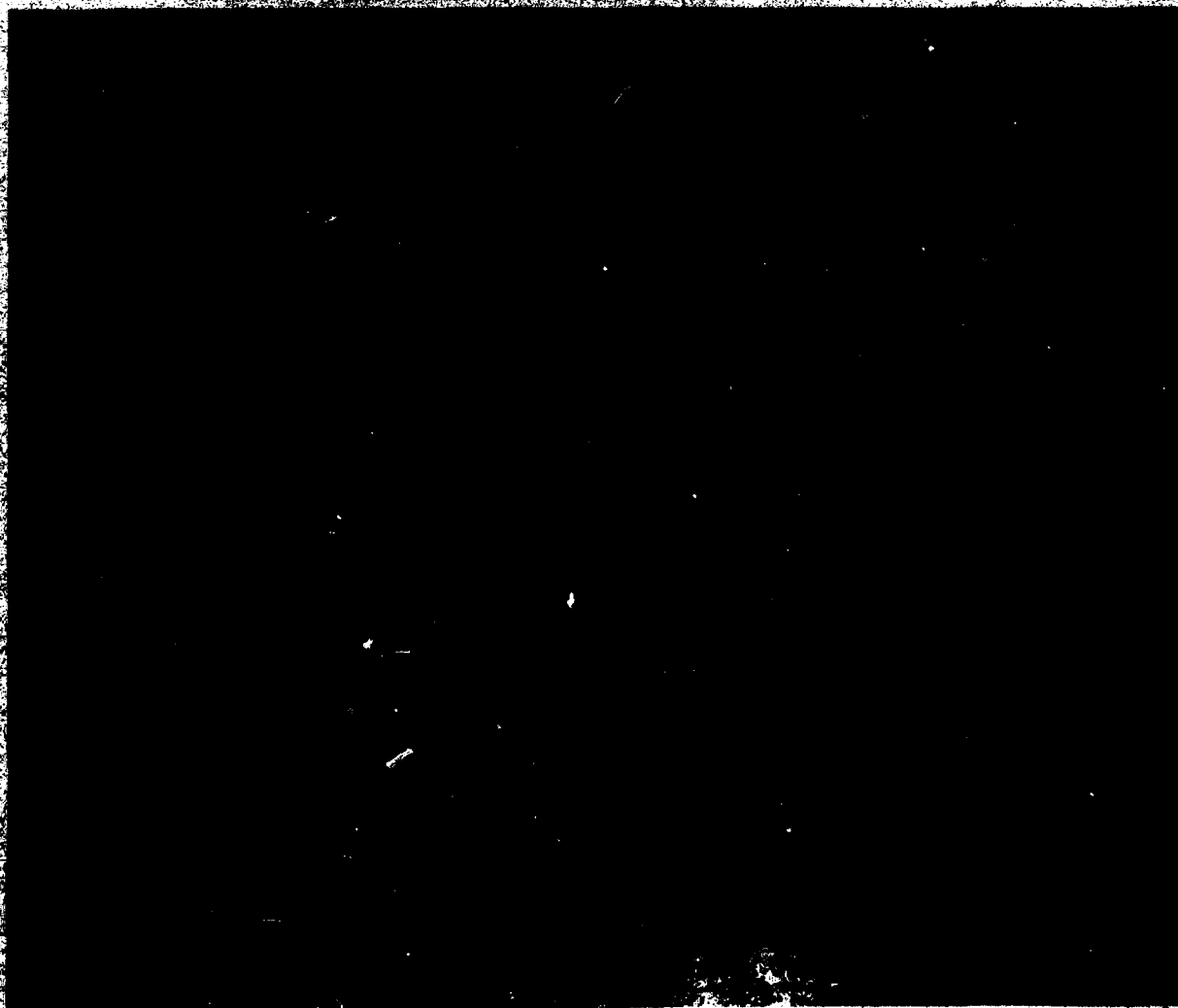
REPORT NO. 124556

JANUARY 1991

UILL-ENG 81-2238

COORDINATED SCIENCE LABORATORY

**CHIP WAVEFORM SELECTION
IN OFFSET-QUATERNARY
DIRECT-SEQUENCE SPREAD-
SPECTRUM MULTIPLE-ACCESS
COMMUNICATIONS**



UNIVERSITY OF ILLINOIS AT URBANA-CHAMPAIGN

83 02 015 080

UNCLASSIFIED

SECURITY CLASSIFICATION OF THIS PAGE (When Data Entered)

REPORT DOCUMENTATION PAGE		READ INSTRUCTIONS BEFORE COMPLETING FORM
1. REPORT NUMBER	2. GOVT ACCESSION NO. <i>AD-A124 556</i>	3. RECIPIENT'S CATALOG NUMBER
4. TITLE (and Subtitle) Chip Waveform Selection in Offset-Quaternary Direct-Sequence Spread-Spectrum Multiple-Access Communications		5. TYPE OF REPORT & PERIOD COVERED Technical Report
7. AUTHOR(s) James Stanley Lehnert		6. PERFORMING ORG. REPORT NUMBER R-907; UILU-ENG 81-2238
		8. CONTRACT OR GRANT NUMBER(s) DAAG29-78-G-0114
9. PERFORMING ORGANIZATION NAME AND ADDRESS Coordinated Science Lab., 1101 W. Springfield Ave. University of Illinois at Urbana-Champaign Urbana, Illinois 61801		10. PROGRAM ELEMENT, PROJECT, TASK AREA & WORK UNIT NUMBERS
11. CONTROLLING OFFICE NAME AND ADDRESS U.S. Army Research Office Research Triangle Park, NC 27709		12. REPORT DATE January 1981
		13. NUMBER OF PAGES 49
14. MONITORING AGENCY NAME & ADDRESS (if different from Controlling Office)		15. SECURITY CLASS. (of this report) Unclassified
		15a. DECLASSIFICATION/DOWNGRADING SCHEDULE
16. DISTRIBUTION STATEMENT (of this Report) Approved for public release; distribution unlimited.		
17. DISTRIBUTION STATEMENT (of the abstract entered in Block 20, if different from Report)		
18. SUPPLEMENTARY NOTES		
19. KEY WORDS (Continue on reverse side if necessary and identify by block number) Spread-Spectrum Multiple-Access Communications Pulse-Shaping for Bandwidth Compression Constant-Envelope Signals		
20. ABSTRACT (Continue on reverse side if necessary and identify by block number) An offset-quaternary direct-sequence spread-spectrum multiple-access communication system is analyzed. This analysis considers the effect of the choice of chip waveforms on the bandwidth which the system utilizes, the signal-to-noise ratio at each user's receiver, and the constant-envelope character of the transmitted signals.		

UILU-ENG 81-2238

CHIP WAVEFORM SELECTION IN OFFSET-QUATERNARY
DIRECT-SEQUENCE SPREAD-SPECTRUM MULTIPLE-ACCESS COMMUNICATIONS

by

James Stanley Lehnert

This work was supported by the Army Research Office under Grant
DAAG29-78-G-0114.

Reproduction in whole or in part is permitted for any purpose of the
United States Government.

Approved for public release. Distribution unlimited.

Accession For	
NTIS GRA&I	<input checked="checked" type="checkbox"/>
DTIC TAB	<input type="checkbox"/>
Unannounced	<input type="checkbox"/>
Justification	
By _____	
Distribution/	
Availability Codes	
Dist. Avail and/or	Special
A	



CHIP WAVEFORM SELECTION IN OFFSET-QUATERNARY
DIRECT-SEQUENCE SPREAD-SPECTRUM MULTIPLE-ACCESS COMMUNICATIONS

BY

JAMES STANLEY LEHNERT

B.S., University of Illinois, 1978

THESIS

Submitted in partial fulfillment of the requirements
for the degree of Master of Science in Electrical Engineering
in the Graduate College of the
University of Illinois at Urbana-Champaign, 1981

Urbana, Illinois

CHIP WAVEFORM SELECTION IN OFFSET-QUATERNARY
DIRECT-SEQUENCE SPREAD-SPECTRUM MULTIPLE-ACCESS COMMUNICATIONS

by

James Stanley Lehnert
Coordinated Science Laboratory and
Department of Electrical Engineering
University of Illinois at Urbana-Champaign

ABSTRACT

An offset-quaternary direct-sequence spread-spectrum multiple-access communication system is analyzed. This analysis considers the effect of the choice of chip waveforms on the bandwidth which the system utilizes, the signal-to-noise ratio at each user's receiver, and the constant-envelope character of the transmitted signals.

ACKNOWLEDGEMENTS

The author is grateful for the constant support and for the advice of his advisor, Professor M. B. Pursley.

Thanks are due to Mrs. Phyllis Young and Mrs. Christine Jewell for their expert and speedy typing.

TABLE OF CONTENTS

CHAPTER	Page
1. INTRODUCTION	1
2. OFFSET-QUATERNARY DS/SSMA SYSTEM ANALYSIS.....	2
2.1 System Model.....	2
2.2 Signal-to-Noise Ratio Analysis.....	7
3. THE CHOICE OF A CHIP WAVEFORM.....	13
3.1 Problem Definition.....	13
3.2 Approximations and Simplifications.....	14
3.2.1 Expected Spectral Density of the k-th User's Transmitted Signal.....	15
3.2.2 Expected SNR at the i-th Receiver.....	18
3.3 A Useful Expression for $\bar{m}_{k,i}^*$	19
3.4 Simple Example Illustrating System Trade-Offs.....	20
3.5 Choice of the Chip Waveform for a Desired Bandwidth.....	21
3.5.1 Minimization of \bar{m}^* with a Constraint Removed.....	22
3.5.2 Approximate Minimization of \bar{m}^* with the Constraint Added.....	24
3.6 The Class of Constant-Envelope Signals.....	29
4. NUMERICAL RESULTS.....	33
5. CONCLUSIONS.....	44
REFERENCES.....	45

CHAPTER 1

INTRODUCTION

The signal-to-noise ratio (SNR) of a biphas direct-sequence spread-spectrum multiple-access (DS/SSMA) communication system has been found in [11] and [12]. This system utilizes a binary phase-shift-keyed modulation type. Conventional digital communication systems utilize other forms of modulation advantageously. It is of interest then to extend the analysis of [11] and [12] to new types of modulation. A DS/SSMA communication system with offset quadriphase-shift-keyed (OQPSK) modulation was analyzed in [4]. The knowledge of the effects of other types of modulation in an SSMA system was thus extended.

We find that we can also extend the analysis to minimum-shift-keyed (MSK) modulation, and by so doing we obtain improvements in both the SNR and the 99 percent power bandwidth of a DS/SSMA communication system [1], [2]. A natural generalization is to consider the performance of a DS/SSMA communication system when a type of modulation is chosen from a class which includes OQPSK and MSK modulations.

We carry out a general analysis of an offset-quaternary direct-sequence spread-spectrum multiple-access (OQ/DS/SSMA) system and examine the considerations involved in choosing a type of modulation from a class. Choosing a modulation type corresponds to choosing a chip waveform, which will shortly be defined. We choose it considering the effects of this choice on the system bandwidth, the SNR at each user's receiver, and the constant-envelope character of the transmitted signals. We also allow the different users in the system to utilize different chip waveforms, and hence have different types of modulation.

CHAPTER 2

OFFSET-QUATERNARY DS/SSMA SYSTEM ANALYSIS

2.1 System Model

Let $p_T(t)$ be the unit rectangular pulse function defined as

$$p_T(t) = \begin{cases} 1, & 0 \leq t < T \\ 0, & \text{otherwise} \end{cases},$$

and let $(b_\ell^{(n)})$ be the n -th, $n \in \{1, \dots, 2K\}$, binary data sequence (i.e., $b_\ell^{(n)} \in \{+1, -1\}$ for each ℓ). The n -th binary data signal is then given by

$$b_n(t) = \sum_{\ell=-\infty}^{\infty} b_\ell^{(n)} p_T(t - \ell T). \quad (2.1)$$

Let $\psi_n(t)$ be the n -th, $n \in \{1, \dots, 2K\}$, chip waveform, a signal which is time-limited to $[0, T_c]$ and which is normalized to satisfy

$$\frac{1}{T_c} \int_0^{T_c} \psi_n^2(t) dt = 1.$$

Notice that in this analysis each binary data sequence is transmitted with a possibly different chip waveform. Let $(a_j^{(n)})$ be the n -th, $n \in \{1, \dots, 2K\}$, binary signature sequence (i.e., $a_j^{(n)} \in \{+1, -1\}$ for each j), which repeats with period $N = T/T_c$. The n -th spectral spreading signal is then given by

$$a_n(t) = \sum_{j=-\infty}^{\infty} a_j^{(n)} \psi_n(t - jT_c). \quad (2.2)$$

Notice that a complete period of a signature sequence occurs during any bit interval of duration T .

The OQ/DS/SSMA communication system for K users transmitting equal power is shown in Figure 2.1. The analysis is easily modified at the final stages when transmitted power varies among users. The transmitted signal for the k -th user is the sum of an in-phase and quadrature component

$$s_k(t) = s_k^I(t) + s_k^Q(t), \quad (2.3)$$

where

$$s_k^I(t) = A a_{2k}(t - t_0) b_{2k}(t - t_0) \cos(\omega_c t + \theta_k) \quad (2.4)$$

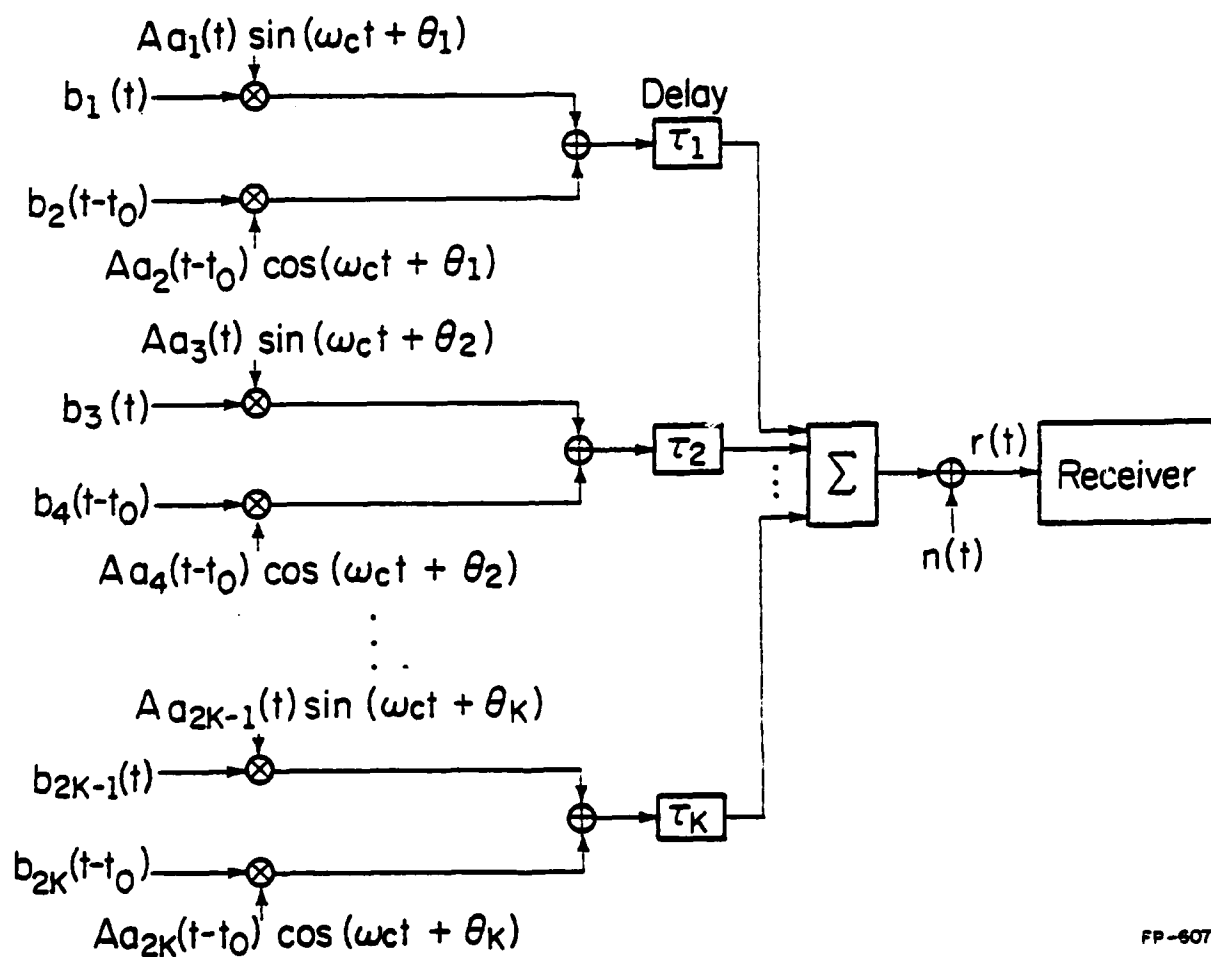
and

$$s_k^Q(t) = A a_{2k-1}(t) b_{2k-1}(t) \sin(\omega_c t + \theta_k). \quad (2.5)$$

Note that ω_c is the angular carrier frequency and that $\omega_c \neq 2\pi/T_c$.

Throughout the analysis $t_0 = \frac{1}{2} \nu T_c$ for some integer ν . If $t_0 = \nu T_c$ for some integer ν and $\psi_k(t) = p_{T_c}(t)$ for $k \in \{1, \dots, 2K\}$, then the DS/SSMA system has quadriphase-shift-keyed (QPSK) modulation. Now suppose $t_0 = \frac{1}{2}(2\nu + 1)T_c$ for some integer ν . If $\psi_k(t) = p_{T_c}(t)$ for $k \in \{1, \dots, 2K\}$, then the system has staggered quadriphase-shift-keyed (SQPSK) modulation, and if $\psi_k(t) = \sqrt{2} \sin(\pi t/T_c) p_{T_c}(t)$ for $k \in \{1, \dots, 2K\}$, then the system has minimum-shift-keyed (MSK) modulation.

The system model assumes a random delay τ_k and a random carrier phase θ_k for each user k , $k \in \{1, \dots, K\}$. It is assumed that the τ_k , for $k \in \{1, \dots, K\}$ are independent identically distributed random variables with distribution which is uniform on $[0, T]$ and that the θ_k for $k \in \{1, \dots, K\}$ are independent identically distributed random variables with distribution which is uniform on $[0, 2\pi]$. This is done because we are



FP-6070

Figure 2.1. OQ/DS/SSMA Communication System Model

concerned with phase angles modulo 2π and with time delays modulo T . Each binary data sequence is modeled as a sequence of identically distributed random variables taking values in $\{-1, +1\}$ with equal probability; $b_\ell^{(j)}$ and $b_n^{(k)}$ are assumed independent whenever $j \neq k$ or $\ell \neq n$. If $\underline{\tau} = [\tau_1, \dots, \tau_K]$, $\underline{\theta} = [\theta_1, \dots, \theta_K]$, and \underline{b} is any vector of finite dimension whose components are elements of the binary data sequences of any of the users, then we assume \underline{b} , $\underline{\tau}$, and $\underline{\theta}$ are independent random vectors. In the analysis we are concerned with $\underline{\varphi} = (\underline{\theta} - \omega_c \underline{\tau}) \pmod{2\pi}$. Given \underline{b} , $\underline{\tau}$, and $\underline{\theta}$ are independent with the given distributions, it follows [2] that \underline{b} , $\underline{\tau}$, and $\underline{\varphi}$ are independent and that the components of $\underline{\varphi}$ are independent identically distributed random variables with distribution which is uniform on $[0, 2\pi]$. The noise process $n(t)$ is assumed to be additive white Gaussian noise with two-sided spectral density $\frac{1}{2} N_0$. It arises from thermal effects which are independent of physical phenomena influencing the other random variables in the model.

The i -th receiver is a correlation receiver consisting of a branch matched to $s_i^I(t)$ and another branch matched to $s_i^Q(t)$. The i -th receiver is shown in Figure 2.2. In the analysis we assume the i -th receiver is synchronized to the i -th transmitted signal. Since in the analysis of the i -th receiver we are concerned with each τ_k and each θ_k relative to τ_i and θ_i , respectively, we may for convenience assume $\tau_i = \theta_i = 0$.

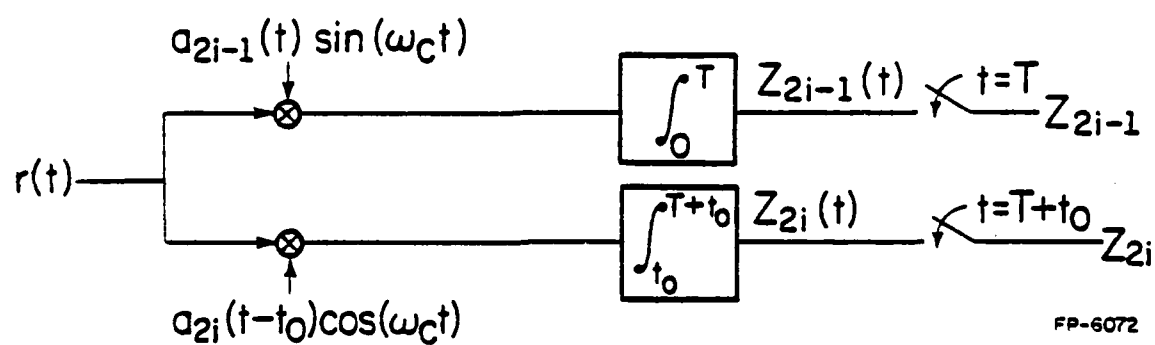


Figure 2.2. Correlation Receiver for the i -th User

2.2 Signal-to-Noise Ratio Analysis

In the analysis of the i -th receiver we can consider the combined random signals of all but the i -th transmitter as noise and thus compute a signal-to-noise ratio (SNR) for each receiver branch. We first consider the quadrature branch. The received signal is given by

$$r(t) = n(t) + \sum_{k=1}^K A a_{2k-1}(t - \tau_k) b_{2k-1}(t - \tau_k) \sin(\omega_c t + \varphi_k) + \sum_{k=1}^K A a_{2k}(t - t_0 - \tau_k) b_{2k}(t - t_0 - \tau_k) \cos(\omega_c t + \varphi_k). \quad (2.6)$$

The output statistic Z_{2i-1} is given by

$$Z_{2i-1} = \int_0^T r(t) a_{2i-1}(t) \sin(\omega_c t) dt. \quad (2.7)$$

Since $\omega_c \gg T^{-1}$, $\int_0^T \frac{1 - \cos(2\omega_c t)}{2} dt \approx T/2$. We can simplify the expression for Z_{2i-1} using this and similar approximations. Remembering $\tau_i = \theta_i = 0$, we have

$$Z_{2i-1} = \eta_{2i-1} + \frac{1}{2} AT [b_0^{(2i-1)} + I], \quad (2.8)$$

where

$$\eta_{2i-1} = \int_0^T n(t) a_{2i-1}(t) \sin(\omega_c t) dt \quad (2.9)$$

and

$$I = \frac{1}{T} \sum_{\substack{k=1 \\ k \neq i}}^K \{ \cos \varphi_k \int_0^T b_{2k-1}(t - \tau_k) a_{2k-1}(t - \tau_k) a_{2i-1}(t) dt + \sin(-\varphi_k) \int_0^T b_{2k}(t - t_0 - \tau_k) a_{2k}(t - t_0 - \tau_k) a_{2i-1}(t) dt \}. \quad (2.10)$$

Letting $x = (t_0 + \tau_k) \pmod T$ and $\mu = (t_0 + \tau_k - x)/T$, we have

$$\begin{aligned}
I = \frac{1}{T} \sum_{\substack{k=1 \\ k \neq i}}^K \left\{ \cos \varphi_k \left[b_{-1}^{(2k-1)} \int_0^{\tau_k} a_{2k-1}(t-\tau_k) a_{2i-1}(t) dt \right. \right. \\
\left. \left. + b_0^{(2k-1)} \int_{\tau_k}^T a_{2k-1}(t-\tau_k) a_{2i-1}(t) dt \right] \right. \\
\left. + \sin(-\varphi_k) \left[b_{-1-\mu}^{(2k)} \int_0^x a_{2k}(t-x) a_{2i-1}(t) dt \right. \right. \\
\left. \left. + b_{-\mu}^{(2k)} \int_x^T a_{2k}(t-x) a_{2i-1}(t) dt \right] \right\} \quad (2.11)
\end{aligned}$$

and

$$\begin{aligned}
I = \frac{1}{T} \sum_{\substack{k=1 \\ k \neq i}}^K \left\{ \cos \varphi_k \left[b_{-1}^{(2k-1)} R_{2k-1,2i-1}(\tau_k) + b_0^{(2k-1)} \hat{R}_{2k-1,2i-1}(\tau_k) \right] \right. \\
\left. + \sin(-\varphi_k) \left[b_{-1-\mu}^{(2k)} R_{2k,2i-1}(x) + b_{-\mu}^{(2k)} \hat{R}_{2k,2i-1}(x) \right] \right\}, \quad (2.12)
\end{aligned}$$

where the continuous-time partial crosscorrelation functions are defined by

$$R_{n,m}(\tau) = \int_0^{\tau} a_n(t-\tau) a_m(t) dt \quad (2.13)$$

and

$$\hat{R}_{n,m}(\tau) = \int_{\tau}^T a_n(t-\tau) a_m(t) dt. \quad (2.14)$$

Since $E\{I\} = 0$, $\text{Var}\{I\} = E\{I^2\}$. Using the independence and the distributions of the random variables mentioned earlier, we have

$$\begin{aligned}
\text{Var}\{I\} = \frac{1}{2T^3} \sum_{\substack{k=1 \\ k \neq i}}^K \int_0^T R_{2k-1,2i-1}^2(\tau) + \hat{R}_{2k-1,2i-1}^2(\tau) \\
+ R_{2k,2i-1}^2(\tau) + \hat{R}_{2k,2i-1}^2(\tau) d\tau \quad (2.15)
\end{aligned}$$

and

$$\text{Var}\{I\} = \frac{1}{2T^3} \sum_{\substack{k=1 \\ k \neq 2i, 2i-1}}^{2K} m_{k,2i-1} + \hat{m}_{k,2i-1} \quad , \quad (2.16)$$

where

$$m_{k,i} = \int_0^T R_{k,i}^2(\tau) d\tau \quad (2.17)$$

and

$$\hat{m}_{k,i} = \int_0^T \hat{R}_{k,i}^2(\tau) d\tau \quad . \quad (2.18)$$

Defining the aperiodic crosscorrelation function

$$C_{k,i}(\ell) = \begin{cases} \sum_{j=0}^{N-1-\ell} a_j^{(k)} a_{j+\ell}^{(i)} , & 0 \leq \ell \leq N-1 \\ \sum_{j=0}^{N-1+\ell} a_{j-\ell}^{(k)} a_j^{(i)} , & 1-N \leq \ell < 0 \\ 0 , & |\ell| \geq N \end{cases} \quad (2.19)$$

and the partial crosscorrelation functions for the chip waveform

$$R_{m,n}^\psi(s) = \int_0^s \psi_m(t+T_c-s) \psi_n(t) dt, \quad 0 \leq s \leq T_c \quad (2.20)$$

and

$$\hat{R}_{m,n}^\psi = \int_s^{T_c} \psi_m(t-s) \psi_n(t) dt, \quad 0 \leq s \leq T_c, \quad (2.21)$$

we can write

$$R_{k,i}(\tau) = C_{k,i}(\ell-N) \hat{R}_{k,i}^\psi(\tau-\ell T_c) + C_{k,i}(\ell+1-N) R_{k,i}^\psi(\tau-\ell T_c) \quad (2.22)$$

and

$$\hat{R}_{k,i}(\tau) = C_{k,i}(\ell) \hat{R}_{k,i}^\psi(\tau-\ell T_c) + C_{k,i}(\ell+1) R_{k,i}^\psi(\tau-\ell T_c), \quad (2.23)$$

where $0 \leq \tau < T$ and $\ell = \lfloor \tau/T_c \rfloor$. We can now simplify (2.17) and (2.18)

by writing

$$\begin{aligned}
 m_{k,i} &= \sum_{\ell=0}^{N-1} \int_{\ell T_c}^{(\ell+1)T_c} R_{k,i}^2(\tau) d\tau = \sum_{\ell=0}^{N-1} \int_0^{T_c} R_{k,i}^2(\tau + \ell T_c) d\tau \\
 &= \sum_{\ell=0}^{N-1} \{ C_{k,i}^2(\ell-N) \hat{m}_{k,i}^\psi + 2C_{k,i}(\ell-N) C_{k,i}(\ell+1-N) \eta_{k,i}^\psi + C_{k,i}^2(\ell+1-N) m_{k,i}^\psi \} \\
 &= \sum_{\ell=-N}^{-1} \{ C_{k,i}^2(\ell) \hat{m}_{k,i}^\psi + 2C_{k,i}(\ell) C_{k,i}(\ell+1) \eta_{k,i}^\psi + C_{k,i}^2(\ell+1) m_{k,i}^\psi \} , \quad (2.24)
 \end{aligned}$$

where

$$m_{k,i}^\psi = \int_0^{T_c} [R_{k,i}^\psi(s)]^2 ds, \quad \hat{m}_{k,i}^\psi = \int_0^{T_c} [\hat{R}_{k,i}^\psi(s)]^2 ds, \quad (2.25)$$

and

$$\eta_{k,i}^\psi = \int_0^{T_c} R_{k,i}^\psi(s) \hat{R}_{k,i}^\psi(s) ds. \quad (2.26)$$

Similarly, we have

$$\begin{aligned}
 \hat{m}_{k,i} &= \sum_{\ell=0}^{N-1} \int_0^{T_c} \hat{R}_{k,i}^2(\tau + \ell T_c) d\tau \\
 &= \sum_{\ell=0}^{N-1} \{ C_{k,i}^2(\ell) \hat{m}_{k,i}^\psi + 2C_{k,i}(\ell) C_{k,i}(\ell+1) \eta_{k,i}^\psi + C_{k,i}^2(\ell+1) m_{k,i}^\psi \} . \quad (2.27)
 \end{aligned}$$

Substituting (2.24) and (2.27) into (2.16) yields

$$\text{Var } I = \frac{1}{T^3} \sum_{\substack{k=1 \\ k \neq 2i, 2i-1}}^{2K} \{ \mu_{k,2i-1}(0) \left(\frac{\hat{m}_{k,2i-1}^\psi + m_{k,2i-1}^\psi}{2} \right) + \mu_{k,2i-1}(1) \eta_{k,2i-1}^\psi \}, \quad (2.28)$$

where

$$\mu_{k,i}(n) = \sum_{\ell=1-N}^{N-1} C_{k,i}(\ell) C_{k,i}(\ell+n). \quad (2.29)$$

If we define

$$\sigma_{n,m}^2 = \frac{1}{2T^3} \int_0^T R_{n,m}^2(\tau) + \hat{R}_{n,m}^2(\tau) d\tau, \quad (2.30)$$

we may write from (2.16)

$$\text{Var } I = \sum_{\substack{k=1 \\ k \neq 2i, 2i-1}}^{2K} \sigma_{k, 2i-1}^2, \quad (2.31)$$

and we see that the variance of the multi-user noise at the i -th receiver may be decomposed into the sum of the variances of noise resulting from each branch of each user's transmitter other than the i -th transmitter.

From (2.8), (2.31), and the definition of $n(t)$,

$$\text{Var}[Z_{2i-1} | b_0^{(2i-1)} = +1] = \frac{1}{2} N_0 T + \frac{A^2 T^2}{4} \sum_{\substack{k=1 \\ k \neq 2i, 2i-1}}^{2K} \sigma_{k, 2i-1}^2. \quad (2.32)$$

From (2.8) we can write the signal-to-noise ratio as

$$\text{SNR}_{2i-1} = \frac{1}{2} AT [\text{Var}[Z_{2i-1} | b_0^{(2i-1)} = +1]]^{-\frac{1}{2}}. \quad (2.33)$$

If the energy per data bit is given by

$$\mathcal{E}_b = \int_0^T [s_k^Q(t)]^2 dt = \frac{1}{2} A^2 T, \quad (2.34)$$

algebraic manipulations then yield (letting $j = 2i-1$)

$$\text{SNR}_j = \left\{ \frac{N_0}{2\mathcal{E}_b} + \sum_{\substack{k=1 \\ k \neq 2i, 2i-1}}^{2K} \sigma_{k, j}^2 \right\}^{-\frac{1}{2}} \quad (2.35)$$

and

$$\text{SNR}_j = \left\{ \frac{N_0}{2\mathcal{E}_b} + T^{-3} \sum_{\substack{k=1 \\ k \neq 2i, 2i-1}}^{2K} \left[\mu_{k,j}(0) \left(\frac{\hat{m}_{k,j}^\psi + m_{k,j}^\psi}{2} \right) + \mu_{k,j}(1) m_{k,j}^\psi \right] \right\}^{-\frac{1}{2}}. \quad (2.36)$$

By a similar analysis we may show that (2.35) and (2.36) hold for $j = 2i$.

This is evident without the analysis, however, by replacing θ_i by

$\theta'_i = (\theta_i + \pi/2)$ and noticing that from this new perspective, Z_{2i} with a new t_0 is the same as Z_{2i-1} was from the original perspective.

Finally, it should be noted that for chip waveforms $\psi_k(t)$ and $\psi_i(t)$ which are symmetric about $t = T_c/2$ (i.e., $\psi_k(t + \frac{1}{2} T_c)$ and $\psi_i(t + \frac{1}{2} T_c)$ are even functions),

$$\hat{R}_{k,i}^\psi(s) = R_{k,i}^\psi(T_c - s) \quad (2.37)$$

and

$$\hat{m}_{k,i}^\psi = m_{k,i}^\psi. \quad (2.38)$$

This can be used to simplify (2.36) to

$$\text{SNR}_j = \left\{ \frac{N_0}{2\mathcal{E}_b} + T^{-3} \sum_{\substack{k=1 \\ k \neq 2i, 2i-1}}^{2K} \left[\mu_{k,j}(0) m_{k,j}^\psi + \mu_{k,j}(1) m_{k,j}^\psi \right] \right\}^{-\frac{1}{2}} \quad (2.39)$$

for $j = 2i$ or $j = 2i-1$.

CHAPTER 3

THE CHOICE OF A CHIP WAVEFORM

3.1 Problem Definition

In the analysis of the OQ/DS/SSMA communication system, we have required each chip waveform $\psi_k(t)$, $k \in \{1, \dots, 2K\}$, to be time limited to $[0, T_c]$. If this restriction were not made, there would be intersymbol interference at the i -th receiver, even if all but the i -th transmitter quit transmitting, and the analysis would be more complicated. In addition we have for convenience imposed a normalization constraint, $\frac{1}{T_c} \int_0^{T_c} \psi_k^2(t) dt = 1$. A large family of chip waveforms which satisfy these conditions remain, and we are left with the problem of choosing a chip waveform. We would like to choose the chip waveform to simultaneously optimize the three system characteristics mentioned in the following paragraphs while satisfying the two constraints already mentioned.

A. Bandwidth

If we assume that outside the frequency range in which the SSMA communication system operates are conventional users who compete for bandwidth, the bandwidth the system utilizes should be as small as possible. The measure of bandwidth which we will use is the 99 percent power bandwidth, which is defined as the frequency range which contains 99 percent of the transmitted energy.

B. Peak Transmitted Power

Transmitters are constrained to operate below a certain peak power threshold in addition to being constrained to operate below an average power level. The maximum allowed average power level, which maximizes the

transmitted energy per bit, may not be attainable unless the envelope of the total transmitted signal is constant. This is true, for example, when the peak power threshold equals the maximum average power level. Additionally, the constant-envelope characteristic of the total transmitted signal is desirable if the signal is to be amplified by a nonlinear amplifier. If the amplitude is constant, the signal will not be distorted in amplitude by the nonlinearity.

C. Signal-to-Noise Ratio

The SNR given in (2.36) is the performance index for the OQ/DS/SSMA communication system which we would like to maximize .

3.2 Approximations and Simplifications

Both the bandwidth which the SSMA communication system utilizes and the SNR at a user's receiver are influenced by not only the chip waveforms, but also the signature sequences which are used in the system. In this chapter we will assume that the periodic binary signature sequences which are used in the system are approximated by random binary sequences as described in [3]. We define a random binary sequence (x_j) of length N to be a sequence of N independent identically distributed random variables x_j for which $\Pr\{x_j = +1\} = \Pr\{x_j = -1\} = \frac{1}{2}$. Each binary vector $\underline{a}^{(k)}$ for $k \in \{1, \dots, 2K\}$ is modelled as a random binary sequence of length N . We assume the vector $\underline{a}^{(k)}$ is independent of $\underline{a}^{(j)}$ for $j \neq k$ and the vectors $\underline{\tau}$, $\underline{\theta}$, and \underline{b} , which were defined earlier. With this model we compute an expected spectral density of any user's transmitted signal which depends solely on the chip waveforms chosen for that user. In addition, only the choice of the chip waveforms remains to influence the SNR.

In much of this chapter we are concerned with the special case in which there is a common chip waveform used throughout the system. This chip waveform $\psi(t)$ is symmetric about $T_c/2$. By this we mean $\psi(t + \frac{1}{2}T_c)$ is an even function of t .

3.2.1 Expected Spectral Density of the k-th User's Transmitted Signal

Let $\gamma(n)$ denote $\left[\frac{n}{N}\right]$. From (2.3), (2.4), and (2.5) we write the k-th transmitted signal as

$$s_k(t) = s_k^I(t) + s_k^Q(t) , \quad (3.1)$$

where

$$s_k^I(t) = A \sum_{n=-\infty}^{\infty} a_n^{(2k)} b_{\gamma(n)}^{(2k)} \psi_{2k}(t - t_0 - nT_c) \cos(\omega_c t + \theta_k) \quad (3.2)$$

and

$$s_k^Q(t) = A \sum_{n=-\infty}^{\infty} a_n^{(2k-1)} b_{\gamma(n)}^{(2k-1)} \psi_{2k-1}(t - nT_c) \sin(\omega_c t + \theta_k) . \quad (3.3)$$

Now we define the baseband components of the transmitted signal as

$$y_{2k}(t) = A \sum_{n=-\infty}^{\infty} a_n^{(2k)} b_{\gamma(n)}^{(2k)} \psi_{2k}(t - t_0 - nT_c) \quad (3.4)$$

and

$$y_{2k-1}(t) = A \sum_{n=-\infty}^{\infty} a_n^{(2k-1)} b_{\gamma(n)}^{(2k-1)} \psi_{2k-1}(t - nT_c) . \quad (3.5)$$

Introducing a random delay T_0 , which is assumed uniformly distributed on $[0, T_c]$ and independent of all other random variables that define the k-th transmitted signal, we can write

$$s_k(t - T_0) = y_{2k}(t - T_0) \cos(\omega_c t + \phi_k') + y_{2k-1}(t - T_0) \sin(\omega_c t + \phi_k') , \quad (3.6)$$

where

$$\varphi'_k = (\theta_k - \omega_c T_0) \pmod{2\pi}. \quad (3.7)$$

We now have a wide-sense-stationary random process, and we may compute its autocorrelation function.

The random variables φ'_k and T_0 are independent, and φ'_k is uniform on $[0, 2\pi]$. This is analogous to φ_k and τ_k being independent and φ_k being uniform on $[0, 2\pi]$ in the system model. Using the mutual independence of \underline{b} , $\underline{a}^{(j)}$ for $j \in \{1, \dots, 2K\}$, T_0 , and φ'_k , where \underline{b} is defined as in the system model, we may write the autocorrelation function of the k -th transmitted signal as

$$\begin{aligned} R_k^T(\tau) &= E\{s_k(t - T_0)s_k(t + \tau - T_0)\} \\ &= \frac{1}{2}[R_k^I(\tau) + R_k^Q(\tau)]\cos \omega_c \tau, \end{aligned} \quad (3.8)$$

where

$$R_k^I(\tau) = E\{y_{2k}(t + \tau - T_0)y_{2k}(t - T_0)\} \quad (3.9)$$

and

$$R_k^Q(\tau) = E\{y_{2k-1}(t + \tau - T_0)y_{2k-1}(t - T_0)\}. \quad (3.10)$$

Substituting (3.5) into (3.10), we find in a manner similar to [5] that

$$\begin{aligned} R_k^Q(\tau) &= A^2 E \left\{ \sum_{n=-\infty}^{\infty} a_n^{(2k-1)} b_{\gamma(n)}^{(2k-1)} \psi_{2k-1}(t + \tau - T_0 - nT_c) \sum_{m=-\infty}^{\infty} a_m^{(2k-1)} b_{\gamma(m)}^{(2k-1)} \psi_{2k-1}(t - T_0 - mT_c) \right\} \\ &= A^2 \sum_{n=-\infty}^{\infty} E \{ [a_n^{(2k-1)} b_{\gamma(n)}^{(2k-1)}]^2 \} E \{ \psi_{2k-1}(t + \tau - T_0 - nT_c) \psi_{2k-1}(t - T_0 - nT_c) \} \end{aligned}$$

$$\begin{aligned}
&= A^2 \sum_{n=-\infty}^{\infty} \frac{1}{T_c} \int_0^{T_c} \psi_{2k-1}(t+\tau-\mu-nT_c) \psi_{2k-1}(t-\mu-nT_c) d\mu \\
&= \frac{A^2}{T_c} \sum_{n=-\infty}^{\infty} \int_{nT_c}^{(n+1)T_c} \psi_{2k-1}(t+\tau-\mu) \psi_{2k-1}(t-\mu) d\mu \\
&= \frac{A^2}{T_c} \int_{-\infty}^{\infty} \psi_{2k-1}(\tau+\mu) \psi_{2k-1}(\mu) d\mu .
\end{aligned} \tag{3.11}$$

If we define $\tilde{\psi}_j(t) = \psi_j(-t)$ for $j \in \{1, \dots, 2K\}$, we may write

$$R_k^Q(\tau) = \frac{A^2}{T_c} \int_{-\infty}^{\infty} \tilde{\psi}_{2k-1}(-\tau-\mu) \psi_{2k-1}(\mu) d\mu, \tag{3.12}$$

and since $R_k^Q(\tau) = R_k^Q(-\tau)$ we have

$$R_k^Q(\tau) = \frac{A^2}{T_c} \int_{-\infty}^{\infty} \tilde{\psi}_{2k-1}(\tau-\mu) \psi_{2k-1}(\mu) d\mu. \tag{3.13}$$

The power spectral density of this baseband signal is given by

$$\begin{aligned}
S_k^Q(\omega) &= \mathcal{F}[R_k^Q(\tau)] \\
&= \frac{A^2}{T_c} |\mathcal{F}[\psi_{2k-1}(t)]|^2,
\end{aligned} \tag{3.14}$$

where \mathcal{F} denotes the Fourier transform. A similar analysis yields

$$R_k^I(\tau) = \frac{A^2}{T_c} \int_{-\infty}^{\infty} \tilde{\psi}_{2k}(\tau-\mu) \psi_{2k}(\mu) d\mu \tag{3.15}$$

and

$$S_k^I(\omega) = \frac{A^2}{T_c} |\mathcal{F}[\psi_{2k}(t)]|^2. \tag{3.16}$$

Returning to (3.8), we can compute the power spectral density

$$S_k^T(\omega) = \mathcal{F}[R_k^T(\tau)] . \quad (3.17)$$

We see that it is just a frequency-shifted version of the sum of two baseband power spectral densities which depend only on the chip waveforms.

3.2.2 Expected SNR at the i -th Receiver

In [3] it is shown that, for independent random sequences $(a_j^{(k)})$ and $(a_j^{(l)})$,

$$E\{C_{k,i}(\ell)C_{k,i}(m)\} = 0 \quad \forall \ell, \forall m: \ell \neq m \quad (3.18)$$

and

$$E\{C_{k,i}^2(\ell)\} = N - |\ell| . \quad (3.19)$$

Returning to (2.29), we see that

$$E\{\mu_{k,i}(1)\} = 0 \quad (3.20)$$

and

$$\begin{aligned} E\{\mu_{k,i}(0)\} &= \sum_{\ell=1-N}^{N-1} N - |\ell| \\ &= N^2 . \end{aligned} \quad (3.21)$$

We can now write (2.36) as

$$SNR_j = \left\{ \frac{N_0}{2\sigma_b^2} + T^{-3} \sum_{\substack{k=1 \\ k \neq 2i, 2i-1}}^{2K} N^2 \tilde{m}_{k,j}^* \right\}^{-\frac{1}{2}} , \quad (3.22)$$

where

$$\bar{m}_{n,m}^{\psi} = \frac{1}{2} (\hat{m}_{n,m}^{\psi} + m_{n,m}^{\psi}), \quad (3.23)$$

and we see that minimizing $\sum_{\substack{k=1 \\ k \neq 2i, 2i-1}}^{2K} \bar{m}_{k,j}^{\psi}$ will maximize the SNR at the

receiver branch corresponding to j .

3.3 A Useful Expression for $\bar{m}_{k,i}^{\psi}$

Let $F_k^{\psi}(\omega) = \mathcal{F}[\psi_k(t)]$ for $k \in \{1, \dots, 2K\}$, where \mathcal{F} denotes the Fourier transform. We will find an expression for $\bar{m}_{k,i}^{\psi}$, where $k, i \in \{1, \dots, 2K\}$, in terms of $F_k^{\psi}(\omega)$ and $F_i^{\psi}(\omega)$.

Remember that $\psi_k(t) = 0$ for $|t| \geq T_c$ and consider the function

$$g_{k,i}(x) = \int_{-\infty}^{\infty} \psi_k(-x+t) \psi_i(t) dt. \quad (3.24)$$

If we examine this function, we find that

$$g_{k,i}(x) = \begin{cases} R_{k,i}^{\psi}(x+T_c) & , \quad -T_c \leq x < 0 \\ \hat{R}_{k,i}^{\psi}(x) & , \quad 0 \leq x \leq T_c \\ 0 & , \quad |x| > T_c. \end{cases} \quad (3.25)$$

From (3.23) and (2.25) we have

$$\bar{m}_{k,i}^{\psi} = \frac{1}{2} \int_0^{T_c} [R_{k,i}^{\psi}(s)]^2 + [\hat{R}_{k,i}^{\psi}(s)]^2 ds. \quad (3.26)$$

However, from (3.25) we may write

$$\bar{m}_{k,i}^{\psi} = \frac{1}{2} \int_{-\infty}^{\infty} g_{k,i}^2(x) dx, \quad (3.27)$$

and defining $G_{k,i}(\omega) = \mathcal{F}[g_{k,i}(x)]$, we have by Parseval's theorem

$$\mathcal{M}_{k,i}^{\psi} = \frac{1}{4\pi} \int_{-\infty}^{\infty} |G_{k,i}(\omega)|^2 d\omega . \quad (3.28)$$

Returning to (3.24), we may write

$$g_{k,i}(x) = \int_{-\infty}^{\infty} \tilde{\psi}_k(x-t) \psi_i(t) dt , \quad (3.29)$$

where $\tilde{\psi}_k(t) = \psi_k(-t)$. Since $g_{k,i}(x)$ is the convolution of $\tilde{\psi}_k(t)$ and $\psi_i(t)$, we have

$$\begin{aligned} G_{k,i}(\omega) &= \mathcal{F}[\tilde{\psi}_k(t)] \mathcal{F}[\psi_i(t)] \\ &= F_k^{\psi}(-\omega) F_i^{\psi}(\omega) . \end{aligned} \quad (3.30)$$

From (3.28) we have

$$\mathcal{M}_{k,i}^{\psi} = \frac{1}{4\pi} \int_{-\infty}^{\infty} |F_k^{\psi}(\omega)|^2 |F_i^{\psi}(\omega)|^2 d\omega . \quad (3.31)$$

This shows that we can decrease the interference to the receiver branch corresponding to i by the transmitter branch corresponding to k by choosing chip pulses which have dissimilar spectral densities.

3.4 A Simple Example which Illustrates the System Trade-Offs

Suppose we let each chip waveform used in the system be the same symmetric (about $T_c/2$) rectangular waveform $\psi(t)$ which is defined as

$$\psi(t) = \begin{cases} \sqrt{\alpha}, & \frac{T_c}{2}(1 - \frac{1}{\alpha}) \leq t \leq \frac{T_c}{2}(1 + \frac{1}{\alpha}) \\ 0, & \text{elsewhere} \end{cases} , \quad (3.32)$$

where $\alpha \geq 1$.

For this chip waveform

$$R_{k,i}^{\psi}(s) = \begin{cases} \alpha t + (1-\alpha)T_c, & T_c(1-\frac{1}{\alpha}) \leq t \leq T_c \\ 0 & , \text{ elsewhere} \end{cases} \quad (3.33)$$

and

$$\hat{R}_{k,i}^{\psi}(s) = R_{k,i}^{\psi}(T_c - s) . \quad (3.34)$$

From (2.25), (3.23), and (3.33)

$$\bar{\eta}_{k,i}^{\psi} = \frac{T_c^3}{3\alpha} . \quad (3.35)$$

For $\alpha = 1$ this system is the standard offset quadriphase SSMA communication system. If α increases beyond 2, $\eta_{k,i}^{\psi} = 0$, and we find that the variance of the multi-user noise I is inversely proportional to α and that the bandwidth of the system is directly proportional to α . The peak power is proportional to $\sqrt{\alpha}$ for $\alpha > 2$.

3.5 Choice of the Chip Waveform for a Desired Bandwidth

In this section we assume that each user is to use the same symmetric chip waveform and that we must contain the transmitted signals in the system within a given 99% power bandwidth. The goal is to maximize the SNR of each user and to accept the peak transmitted power levels which result.

We define $f(t) = \psi(t + T_c/2)$ and $\mathcal{F}[f(t)] = F(\omega)$. Since there is only one chip waveform used in the system, we will simplify the notation by letting $\psi_k(t) = \psi(t)$ for $k \in \{1, \dots, 2K\}$ and defining $\bar{\eta}^{\psi} = \bar{\eta}_{1,1}^{\psi}$. We have $\bar{\eta}_{k,i}^{\psi} = \bar{\eta}^{\psi}$ for any $k, i \in \{1, \dots, 2K\}$.

3.5.1 Minimization of \bar{M}^ψ with a Constraint Removed

From (3.31) we have

$$\begin{aligned}\bar{M}^\psi &= \frac{1}{4\pi} \int_{-\infty}^{\infty} |F_1^\psi(\omega)|^4 d\omega \\ &= \frac{1}{4\pi} \int_{-\infty}^{\infty} |F(\omega)|^4 d\omega ,\end{aligned}\tag{3.36}$$

and since $f(t)$ is an even function,

$$\bar{M}^\psi = \frac{1}{4\pi} \int_{-\infty}^{\infty} F^4(\omega) d\omega .\tag{3.37}$$

For a given bandwidth constraint we would like to minimize \bar{M}^ψ over all choices of $f(t)$ which are time limited to $[-\frac{1}{2} T_c, \frac{1}{2} T_c]$ and hence over all choices of $\psi(t)$ which are time limited to $[0, T_c]$. We cannot have $f(t)$ both strictly band limited and strictly time limited [10]. We first find the minimum of \bar{M}^ψ when f is not time limited and when its Fourier transform $F(\omega)$ vanishes outside the interval $[-\Omega, \Omega]$.

We define $G(\omega) = F^2(\omega)$ and use Jensen's inequality to write

$$\left[\frac{1}{2\Omega} \int_{-\Omega}^{\Omega} g(\omega) d\omega \right]^2 \leq \frac{1}{2\Omega} \int_{-\Omega}^{\Omega} G^2(\omega) d\omega .\tag{3.38}$$

Equality holds in (3.38) if $G(\omega)$ is a constant function on $[-\Omega, \Omega]$. Since $f(t)$ is even, by Parseval's theorem we may write

$$\begin{aligned}\frac{1}{2\pi} \int_{-\Omega}^{\Omega} G(\omega) d\omega &= \int_{-\infty}^{\infty} f^2(t) dt \\ &= T_c .\end{aligned}\tag{3.39}$$

From (3.38) and (3.39) we have

$$\frac{1}{4\pi} \int_{-\Omega}^{\Omega} G^2(\omega) d\omega \geq \frac{\pi T_c^2}{2\Omega}, \quad (3.40)$$

with equality if $G(\omega)$ is constant on $[-\Omega, \Omega]$. From (3.37), (3.40), and the definition of $G(\omega)$ we have

$$\bar{M}^\psi \geq \frac{\pi T_c^2}{2\Omega}, \quad (3.41)$$

with equality if $|F(\omega)|$ is a constant function on $[-\Omega, \Omega]$.

In summary, we have generalized the definition of \bar{M}^ψ to include $\psi(t)$ which are not time limited. When we had $F(\omega)$ strictly limited to the interval $[-\Omega, \Omega]$, we obtained the bound (3.41).

3.5.2 Approximate Minimization of \mathcal{M}^Ψ with the Constraint Added

We now constrain $\psi(t)$ and hence $f(t)$ to be strictly time limited. This is the constraint we have assumed in the system model. We relax the constraint of being strictly band limited. We instead constrain $f(t)$ to have 99 percent of its energy in a given frequency range.

We are guided in our choice of $f(t)$ by the results of the previous section. Since \mathcal{M}^Ψ was minimized there for

$$F(\omega) = k p_\Omega(|\omega|), \quad (3.42)$$

where k is a constant, we find a time-limited function $f(t)$ for which (3.42) nearly holds.

In [6]-[9] the prolate spheroidal wave functions are described. We will state some of the dual results which follow by interchanging the roles of the variables $-f$ and t , where $\omega = 2\pi f$ and the transform pair is specified by

$$F(\omega) = \int_{-\infty}^{\infty} f(t) e^{-j\omega t} dt \quad (3.43)$$

and

$$f(t) = \frac{1}{2\pi} \int_{-\infty}^{\infty} F(\omega) e^{j\omega t} d\omega. \quad (3.44)$$

Following [7], we adopt the notation $\|f(x)\|_A^2 = \int_{-A}^A |f(x)|^2 dx$. We denote by \mathcal{L}_A^2 the class of all complex valued functions $F(-2\pi f)$ on $[-A, A]$ which satisfy $\int_{-A}^A |F(-2\pi f)|^2 df < \infty$. By \mathcal{D} we denote the subclass of \mathcal{L}_∞^2 consisting of the $F(-2\pi f)$ whose inverse Fourier transforms vanish if $|t| > T_c/2$.

Given any $W > 0$ and any $T_c > 0$, we can find a countably infinite set of real functions $\varphi_0(f)$, $\varphi_1(f)$, $\varphi_2(f)$... called the prolate spheroidal wave functions and a set of real positive numbers $\lambda_0 > \lambda_1 > \lambda_2 > \dots$ called the eigenvalues with the following properties:

A. The $\varphi_i(f)$ are time limited, complete in \mathcal{L}_2 , and orthonormal on the real line:

$$\int_{-\infty}^{\infty} \varphi_i(f) \varphi_j(f) df = \begin{cases} 0, & i \neq j \\ 1, & i = j \end{cases} \quad i, j \in \{0, 1, 2, \dots\} \quad (3.45)$$

B. In the interval $-W \leq f \leq W$, the $\varphi_i(f)$ are complete in \mathcal{L}_W^2 and orthogonal:

$$\int_{-W}^W \varphi_i(f) \varphi_j(f) df = \begin{cases} 0, & i \neq j \\ \lambda_i, & i = j \end{cases} \quad i, j \in \{0, 1, 2, \dots\} \quad (3.46)$$

C. For all values of f , real or complex,

$$\lambda_i \varphi_i(f) = \int_{-W}^W \frac{\sin[\pi T_c(t-s)]}{\pi(t-s)} \varphi_i(s) ds, \quad i \in \{0, 1, 2, \dots\}. \quad (3.47)$$

Both the prolate spheroidal wave functions and the corresponding eigenvalues are functions of a normalized bandwidth $b = \pi T_c W$. For a fixed value of b , the λ_i fall off to zero rapidly with increasing i , once i has exceeded $(2/\pi)b = 2T_c W$.

Remember that we have defined $f(t) = \psi(t + T_c/2)$ and $F(\omega) = \mathcal{F}[f(t)]$.

Since $f(t)$ is even, we have

$$F(2\pi f) = F(-2\pi f), \quad (3.48)$$

and since $f(t) = 0$ for $|t| > T_c/2$, we can write

$$F(2\pi f) = \sum_{n=0}^{\infty} A_n \varphi_n(f). \quad (3.49)$$

In what follows we define

$$A(f) = \sum_{n=0}^{\infty} A_n \varphi_n(f). \quad (3.50)$$

Observing (3.37), we would like to find the A_i which minimize

$$\mathcal{M}^{\psi} = \frac{1}{2} \int_{-\infty}^{\infty} \left[\sum_{n=0}^{\infty} A_n \varphi_n(f) \right]^4 df \quad (3.51)$$

when we are subject to the constraint $\|A(f)\|_W^2 = .99T_c$. This is difficult.

Instead we choose the A_i to approximate

$$B(f) = k p_W(|f|), \quad (3.52)$$

where k is some constant. Since the $\varphi_i(f)$ are complete in L_W^2 , we have by (3.46)

$$B(f) = \begin{cases} \sum_{n=0}^{\infty} B_n \varphi_n(f) & , |f| \leq W \\ 0 & , |f| > W \end{cases} \quad (3.53)$$

where

$$B_n = \frac{1}{\lambda_n} \int_{-W}^W k \varphi_n(f) df. \quad (3.54)$$

The function $B(f)$ considered only on $[-W, W]$ is not the transform of a finite-energy time-limited function considered only on $[-W, W]$. This is evident from the following argument. If we assume that it is the transform of a finite-energy time-limited function considered only on $[-W, W]$, then it must be analytic in the entire f plane. However, an analytic function in the entire f plane which is constant on an interval must be a constant function. This cannot be the case because the inverse transform of a constant function of frequency is the unit impulse function. It is not a finite-energy signal. Since $B(f)$ considered on $[-W, W]$ is not the Fourier transform of a finite-energy time-limited function considered on $[-W, W]$, $\sum_{n=0}^N B_n^2$ grows without bound for increasing N . If it did not grow without bound for increasing N , we would have $\sum_{n=0}^{\infty} B_n \varphi_n(f)$, the transform of a finite-energy time-limited function, equal to $B(f)$ on $[-W, W]$.

Returning to (3.49), we attempt to minimize $\|A(f) - B(f)\|_W^2$ while constraining the energy of $A(f)$ for $|f| \geq W$ by the equation

$$\|A(f)\|_{\infty}^2 - \|A(f)\|_W^2 = E. \quad (3.55)$$

Equation (3.55) states that the energy of $f(t)$ outside the frequency range $[-W, W]$ equals the quantity E . We may now begin to calculate the coefficients A_n by writing

$$\|A(f) - B(f)\|_W^2 = \left\| \sum_{n=0}^{\infty} (A_n - B_n) \varphi_n(f) \right\|_W^2. \quad (3.56)$$

From (3.46)

$$\|A(f) - B(f)\|_W^2 = \sum_{n=0}^{\infty} (A_n - B_n)^2 \lambda_n, \quad (3.57)$$

and from (3.46) and (3.55) we have

$$\sum_{n=0}^{\infty} A_n^2 (1 - \lambda_n) = E. \quad (3.58)$$

Using a Lagrange multiplier μ , we may find the coefficients of A_n which minimize (3.57) with the side constraint given by (3.55). We require

$$\frac{\partial}{\partial A_j} \left[\sum_{n=0}^{\infty} (A_n - B_n)^2 \lambda_n + \mu \left(\sum_{n=0}^{\infty} A_n^2 (1 - \lambda_n) - E \right) \right] = 0 \quad (3.59)$$

for $j \in \{0, 1, \dots\}$. The equations (3.58) and (3.59) simplify for $j \in \{0, 1, \dots\}$ to

$$A_j = \frac{B_j \lambda_j}{\lambda_j + \mu(1 - \lambda_j)}, \quad (3.60)$$

where μ , a positive quantity, is given by

$$\sum_{n=0}^{\infty} \frac{B_n^2 \lambda_n^2 (1 - \lambda_n)}{[\mu(1 - \lambda_n) + \lambda_n]^2} = E. \quad (3.61)$$

The total energy of the signal $f(t)$ is T_c , so by Parseval's theorem, (3.45), and (3.60) we have

$$\begin{aligned} \|A\|_{\infty}^2 &= \sum_{n=0}^{\infty} \frac{B_n^2 \lambda_n^2}{[\mu(1 - \lambda_n) + \lambda_n]^2} \\ &= T_c. \end{aligned} \quad (3.62)$$

We choose k in (3.52) to meet this requirement. The constraint that 99 percent of the signal energy is contained in $[-W, W]$ becomes the constraint that $E = .01 T_c$.

The equations (3.60) and (3.61) specify the coefficients A_j in (3.50). If we take the inverse Fourier transform of $A(f)$ we obtain $f(t)$ and therefore $\psi(t)$. This $\psi(t)$ has 99 percent of its energy in $[-W, W]$ and has been chosen to result in a small value of \overline{M}^ψ .

3.6 The Class of Constant-Envelope Signals

In this section we obtain a parametric representation of any two chip waveforms $\psi_1(t)$ and $\psi_2(t)$ which produce a constant-envelope transmitted signal. The chip waveforms $\psi_1(t)$ and $\psi_2(t)$ are used in the quadrature and in-phase branches of the transmitter, respectively. We define for $j = 1$ and $j = 2$

$$\bar{\psi}_j(t) = \sum_{n=-\infty}^{\infty} c_n^{(j)} \psi_j(t - nT_c), \quad (3.63)$$

where $c_n^{(j)}$ is a variable which takes values in $\{-1, +1\}$. We constrain the offset parameter t_0 to satisfy $t_0 = \frac{1}{2}(2\nu + 1)T_c$ in our system model. This allows us to write the envelope of a user's total transmitted signal as

$$e(t) = [\bar{\psi}_1^2(t) + \bar{\psi}_2^2(t - T_c/2)]^{\frac{1}{2}}. \quad (3.64)$$

If the total transmitted signal has a constant envelope, we may write it as

$$s(t) = \sqrt{2} \cos(\omega_c t + \theta + \alpha(t)), \quad (3.65)$$

where $\alpha(t)$ is slowly varying relative to the quantity $\omega_c t$. Expanding this, we have

$$s(t) = \sqrt{2} \cos \alpha(t) \cos(\omega_c t + \theta) - \sqrt{2} \sin \alpha(t) \sin(\omega_c t + \theta) \quad (3.66)$$

We represent $\bar{\psi}_1(t)$ and $\bar{\psi}_2(t)$ parametrically by

$$\bar{\psi}_1(t) = \sqrt{2} \sin \alpha(t) \quad (3.67)$$

and

$$\bar{\psi}_2(t) = \sqrt{2} \cos \alpha(t) \quad (3.68)$$

In (3.67) and (3.68) $\alpha(t)$ has certain restrictions. It must satisfy $\alpha(0) = k\pi$, $k \in I$, where I represents the set of integers, in order to satisfy $\bar{\psi}_1(0) = 0$. During each time interval $[nT_c/2, (n+1)T_c/2]$, $n \in I$, $\alpha(t)$ must undergo a net phase change of $\pi/2$ radians in order for both $\bar{\psi}_1(t)$ to be zero for $t = kT_c$ and $\bar{\psi}_2(t)$ to be zero for $t = \frac{1}{2}(2k+1)T_c$, where $k \in I$. If $k \in I$, we have

$$|\alpha(t) - \alpha(kT_c)| = \beta(t) \text{ for } kT_c \leq t < (\frac{2k+1}{2})T_c \quad (3.69)$$

and

$$|\alpha(t) - \alpha[(\frac{2k+1}{2})T_c]| = \gamma(t) \text{ for } (\frac{2k+1}{2})T_c \leq t < (k+1)T_c, \quad (3.70)$$

where $\beta(t)$ and $\gamma(t)$ are functions satisfying $\beta(0) = \gamma(0) = 0$ and $\beta(T_c/2) = \gamma(T_c/2) = \pi/2$. Equations (3.69) and (3.70) are required since the shape of the chip waveform must not change over time.

We do have flexibility in choosing $\beta(t)$ and $\gamma(t)$. By the identity $\cos(\alpha(t) \pm \pi/2) = \mp \sin \alpha(t)$, we see that the condition $\beta(t) = \gamma(t)$ is equivalent to the condition $\bar{\psi}_1(t) = \bar{\psi}_2(t)$. We see that shaping $\beta(t)$ shapes the left half of $\bar{\psi}_1(t)$ and the right half of $\bar{\psi}_2(t)$. Shaping $\gamma(t)$ shapes the right half of $\bar{\psi}_1(t)$ and the left half of $\bar{\psi}_2(t)$. Although the combined normalization

$$\frac{1}{T_c} \int_0^{T_c} \psi_1^2(t) + \psi_2^2(t) dt = 2 \quad (3.71)$$

is satisfied for all constant-envelope chip waveform pairs, the energy distribution between $\psi_1(t)$ and $\psi_2(t)$ is not always even.

The condition for $\psi_1(t)$ and $\psi_2(t)$ to be symmetric can be found by representing $\psi_1(t)$ by

$$\psi_1(t) = \begin{cases} \sin \beta(t) & , \quad 0 \leq t < T_c/2 \\ \sin[\pi/2 - \gamma(t - T_c/2)] & , \quad T_c/2 \leq t < T_c \end{cases} \quad (3.72)$$

We can now write $f_1(t) = \psi_1(t + T_c/2)$ as

$$f_1(t) = \begin{cases} \sin \beta(t + T_c/2) & , \quad -T_c/2 \leq t < 0 \\ \sin[\pi/2 - \gamma(t)] & , \quad 0 \leq t < T_c/2 \end{cases} \quad (3.73)$$

The condition for symmetry is the condition $f_1(t) = f_1(-t)$ for $t \in [-T_c/2, T_c/2]$. We state this as

$$\sin \beta(T_c/2 - t) = \sin[\pi/2 - \gamma(t)] \quad (3.74)$$

or

$$\beta(T_c/2 - t) = \pi/2 - \gamma(t) \quad (3.75)$$

or

$$\beta'(T_c/2 - t) = \gamma'(t) \quad (3.76)$$

for $t \in [0, T_c/2]$, where $\beta'(\cdot)$ and $\gamma'(\cdot)$ are the first derivatives of $\beta(\cdot)$ and $\gamma(\cdot)$, respectively. When using (3.76), we must remember $\gamma(0) = \beta(0) = 0$. If we had considered $\psi_2(t)$ in (3.72), we would have obtained a similar result.

As examples of our parametric representation of constant-envelope systems, we can consider an SQPSK/SSMA communication system and an MSK/SSMA communication system. For SQPSK $\gamma(t) = \beta(t)$, and $\gamma(t)$ is defined by the fact that $\gamma(0) = 0$ and by its derivative

$$\gamma'(t) = \frac{\pi}{4} \delta(t) + \frac{\pi}{4} \delta(t - T_c/2), \quad (3.77)$$

where $\delta(t)$ is the unit impulse function. For MSK $\gamma(t) = \beta(t)$, and $\gamma(t)$ is defined by the fact that $\gamma(0) = 0$ and by its derivative

$$\gamma'(t) = \pi/T_c, \quad 0 \leq t < T_c/2. \quad (3.78)$$

Notice that these derivatives must satisfy (3.76) for the required symmetry in the chip waveform.

CHAPTER 4

NUMERICAL RESULTS

We use the method described in 3.5.2 to find chip waveforms with good SNR and bandwidth properties. We are aided by the fact that for a fixed value of b , the λ_i fall off to zero rapidly with increasing i , once i has exceeded $(2/\pi)b = 2T_c W$. In other words, for some positive integer L , $\lambda_L \approx 0$ and $0 < \lambda_i < \lambda_L$ for $i > L$. We are trying to find the coefficients A_i in the expansion of $A(f)$, a function which is to have 99 percent of its energy contained in $[-W, W]$. Since λ_i is equal to the fraction of energy which $\varphi_i(f)$ possesses within the frequency interval $[-W, W]$, certainly we can neglect the A_i 's which correspond to λ_i 's which are nearly zero. We are further convinced of this by examining (3.60) and knowing for the case $b = 6$, $\mu \approx 6.85$. We may express the function

$$\begin{aligned} A(f) &= \sum_{n=0}^{\infty} A_n \varphi_n(f) \\ &\approx \sum_{n=0}^L A_n \varphi_n(f) . \end{aligned} \quad (4.1)$$

We solve the integral equation (3.47) numerically and evaluate the coefficients B_n , which are defined in (3.54), for $n \in \{1, \dots, L\}$. We use the B_n to calculate A_n , and since we are only interested in A_n for $n \leq L$, we are only interested in B_n for $n \leq L$. A plot of $\sum_{n=0}^L B_n \varphi_n(f)$ appears in Figure 4.1. This plot was made for $b = 6$, for $k = 1$, and for $L = 8$. We know $\lambda_9 \approx 10^{-7}$. This means only about 10^{-5} percent of the energy of $\varphi_9(f)$ is contained in $[-W, W]$, and we have taken L large enough to get a good approximation to $A(f)$.

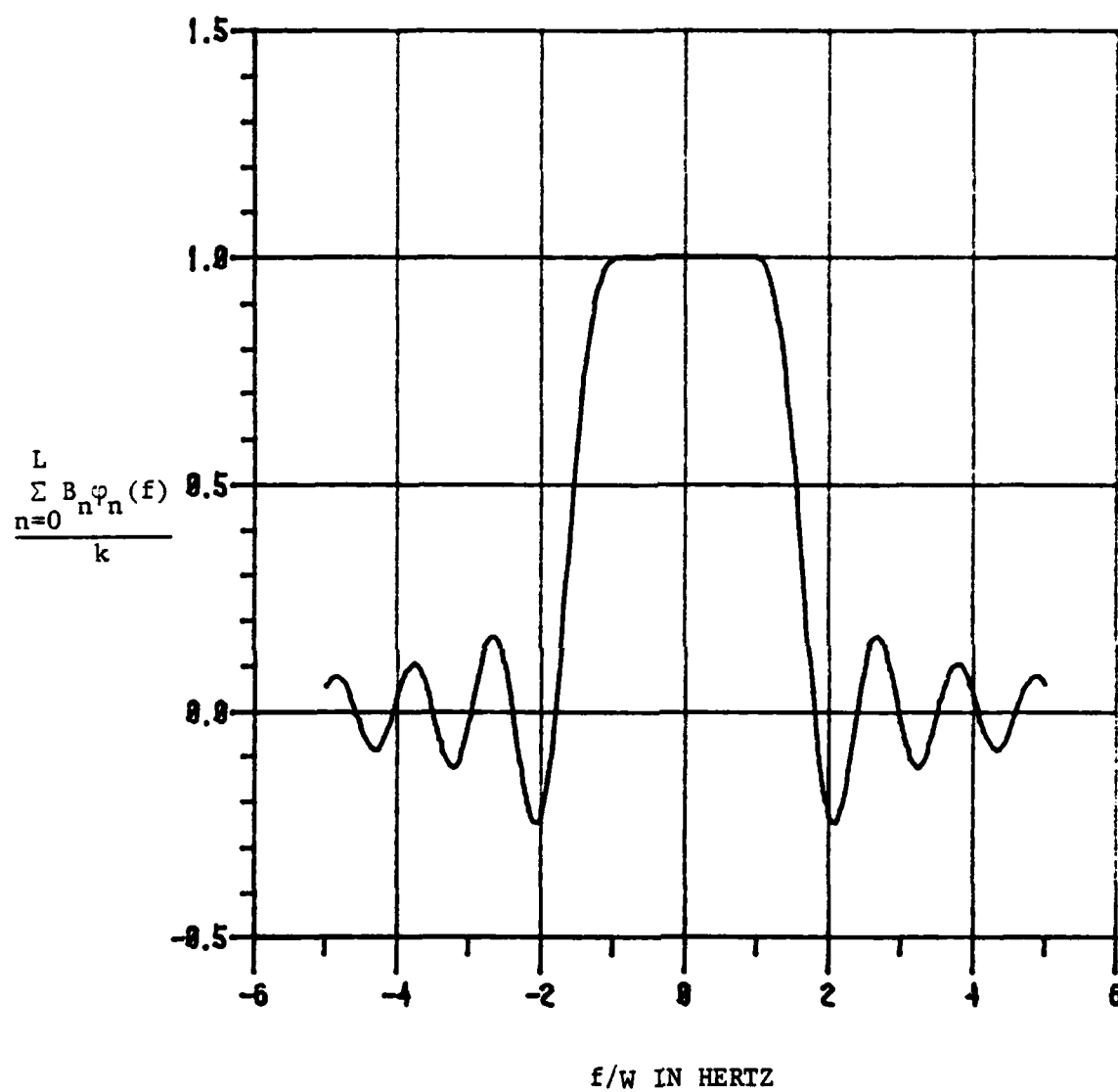


Figure 4.1. $\sum_{n=0}^L B_n \varphi_n(f)$ vs. f/W , ($W = \frac{6}{\pi T_c}$, $L = 8$)

Figure 4.2 shows $A(f)$. We solve the nonlinear equations (3.61) and (3.62) (with $E = .01 T_c$) numerically, find the coefficients A_1 through A_8 defined in (3.60), and plot $\sum_{n=0}^{\infty} A_n \varphi_n(f)$. Notice that the energy outside $[-W, W]$ has been squelched by the 99 percent energy constraint. Figure 4.1 could show much more energy outside $[-W, W]$ if we allowed L to be greater than 8, but Figure 4.2 would still appear much the same.

Finally, we numerically take the inverse Fourier transform of $A(f)$ to find the displaced chip waveform $f(t)$. We call this a pulse with parameter $b = 6$. The result is shown in Figure 4.3. The function $f(t)$ is slightly in error at the endpoints of the interval $[-T_c/2, T_c/2]$ as a result of truncating the evaluation of $f(t)$ to

$$f(t) \approx \int_{-\alpha}^{\alpha} A(f) e^{j2\pi ft} df \quad (4.2)$$

For the case when $b = 6$, we let $\alpha = 10 W$.

Figures 4.4 and 4.5 show the displaced chip waveforms $f(t)$ which result when $b = 3.71$ and $b = 32.28$, respectively. These offset chip waveforms result in the same expected 99 percent power bandwidth as an MSK/SSMA communication system and an OQPSK/SSMA communication system, respectively. Examining Table 4.1, we see that the resulting parameter \bar{m}^\dagger is slightly smaller for the case $b = 3.71$ and much smaller (by a factor of about 14) for the case $b = 32.28$, as compared with the MSK/SSMA and OQPSK/SSMA communication systems, respectively. We also see that for the case $b = 3.71$, the envelope of the total transmitted signal is nearly constant, and for the case $b = 32.28$, the envelope fluctuates greatly. This table illustrates again the trade-offs which the example in section 3.4 illustrates.

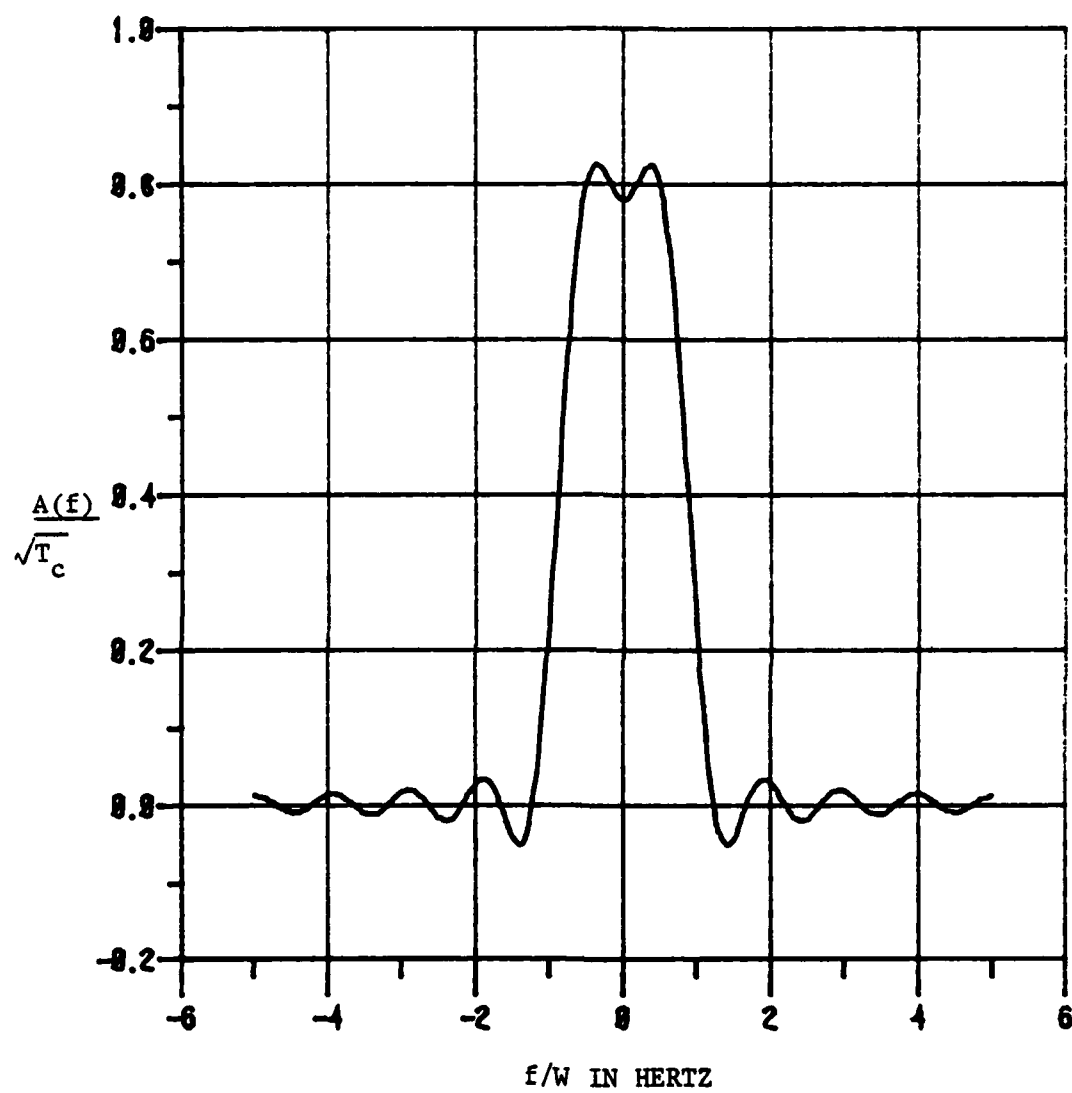


Figure 4.2. $A(f)$ vs. f/W , ($W = \frac{6}{\pi T_c}$, $L = 8$)

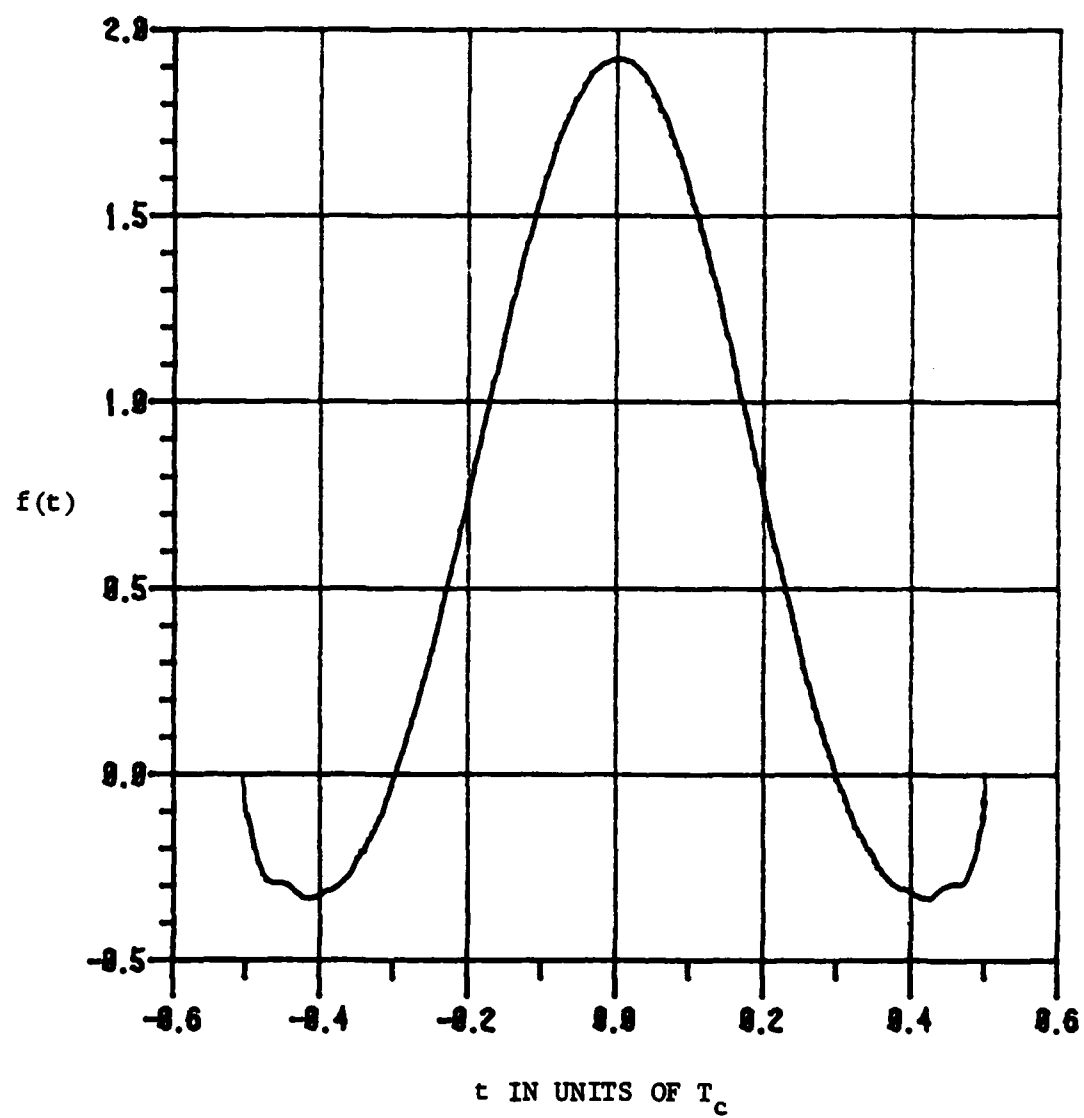


Figure 4.3. $f(t)$ vs. t , ($W = \frac{1.91}{T_c}$)

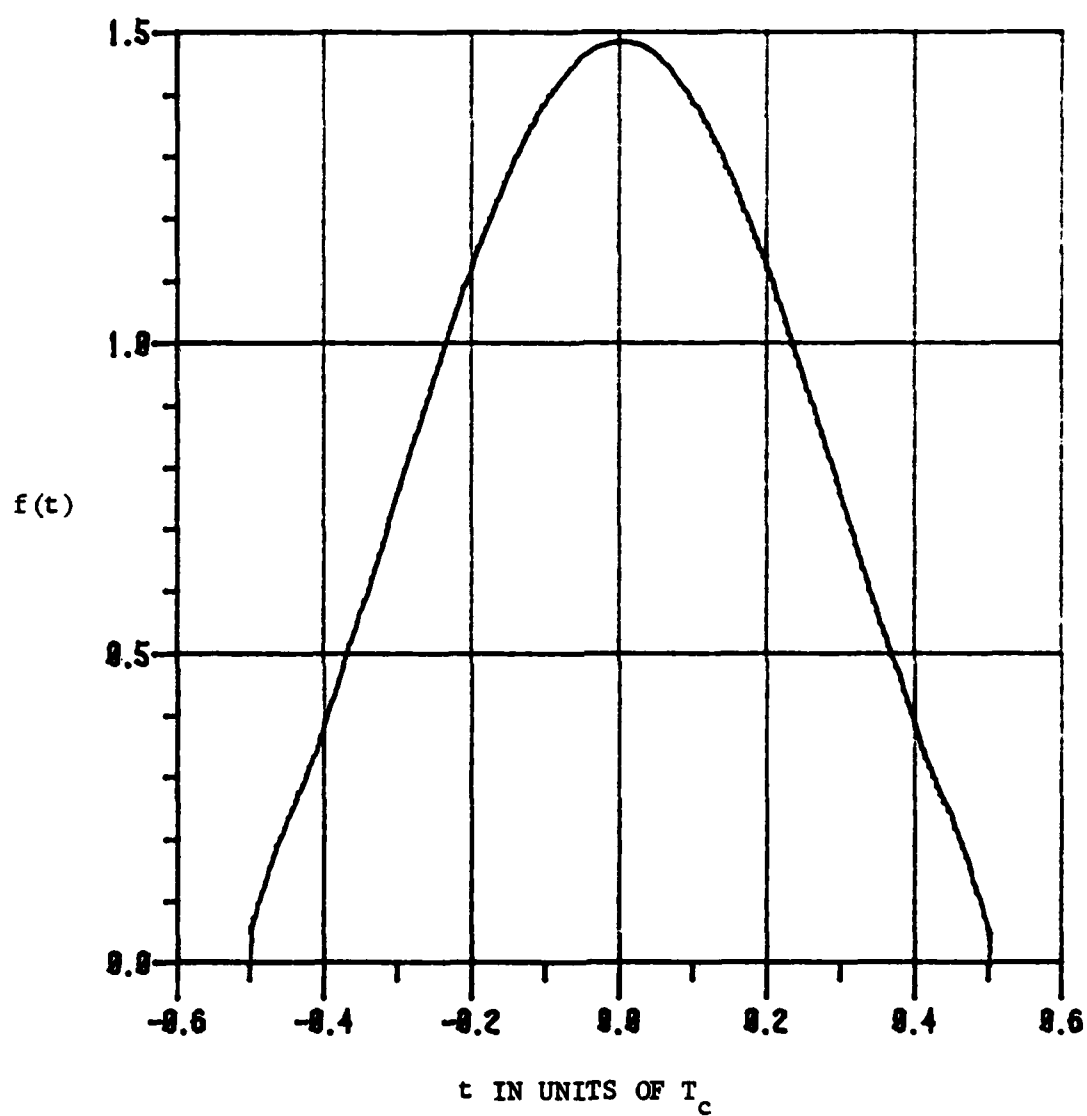


Figure 4.4. $f(t)$ vs. t , ($W = \frac{1.18}{T_c}$)

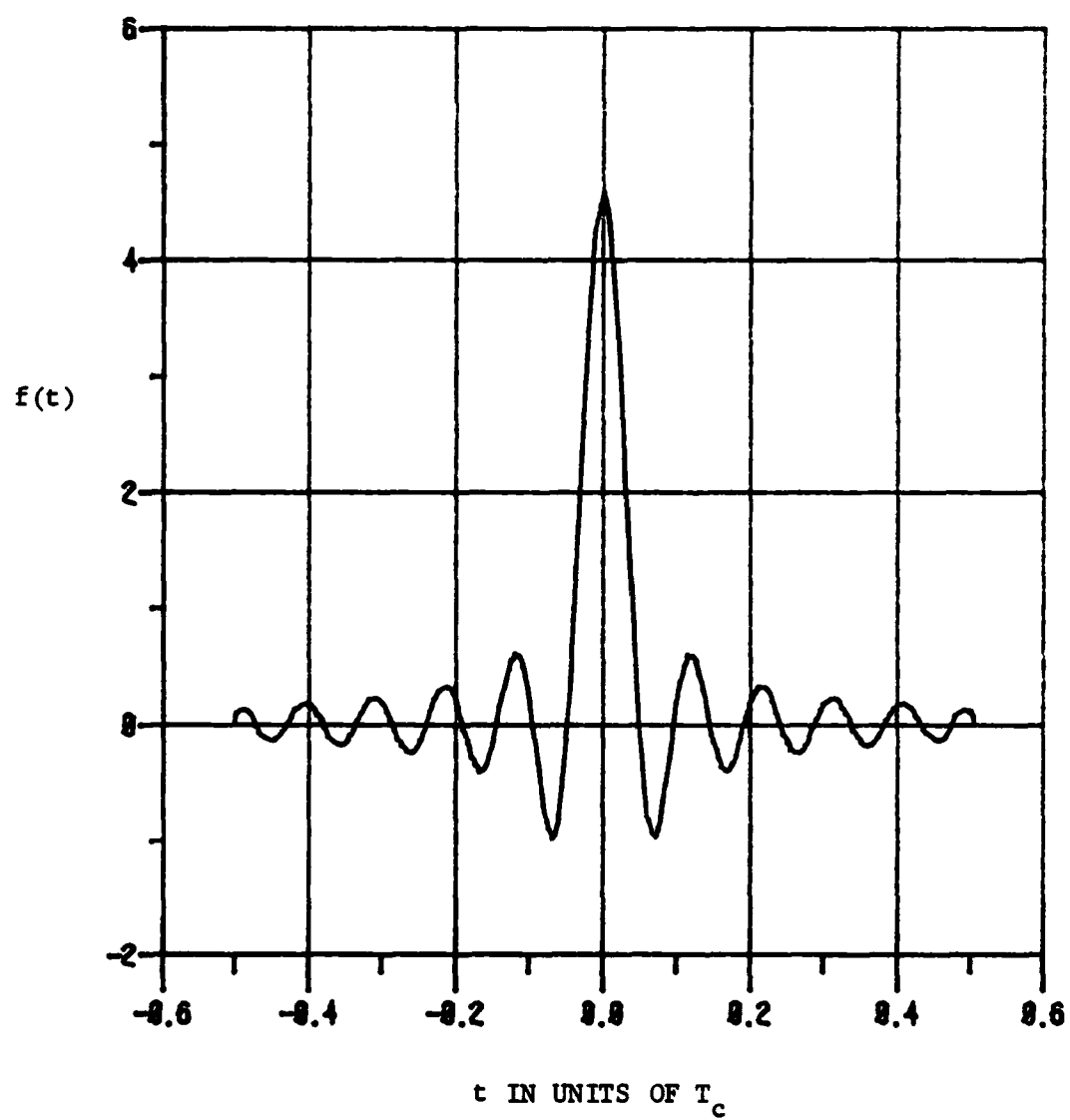


Figure 4.5. $f(t)$ vs. t , ($W = \frac{10.28}{T_c}$)

From the results in 3.2.1, the expected spectral properties of the transmitted signals depend upon the choice of the chip waveforms. We consider the expected fraction of transmitted power which is not contained within a frequency band centered about the carrier frequency ω_c and define ten times the base-ten logarithm of this quantity as the fractional out-of-band power in dB. Figure 4.6 shows the fractional out-of-band power in dB for chip waveforms found using prolate spheroidal functions, and Figure 4.7 shows this quantity for some standard symmetric pulses which are of interest. We see the same effect which we suspected from our derivation in section 3.5.1 if we examine Figure 4.6, Figure 4.7, and Table 4.1 together. The chip waveforms that spread their energy more evenly over the allowed frequency range tend to have a smaller η parameter. This will cause an improved SNR in the SSMA communication system.

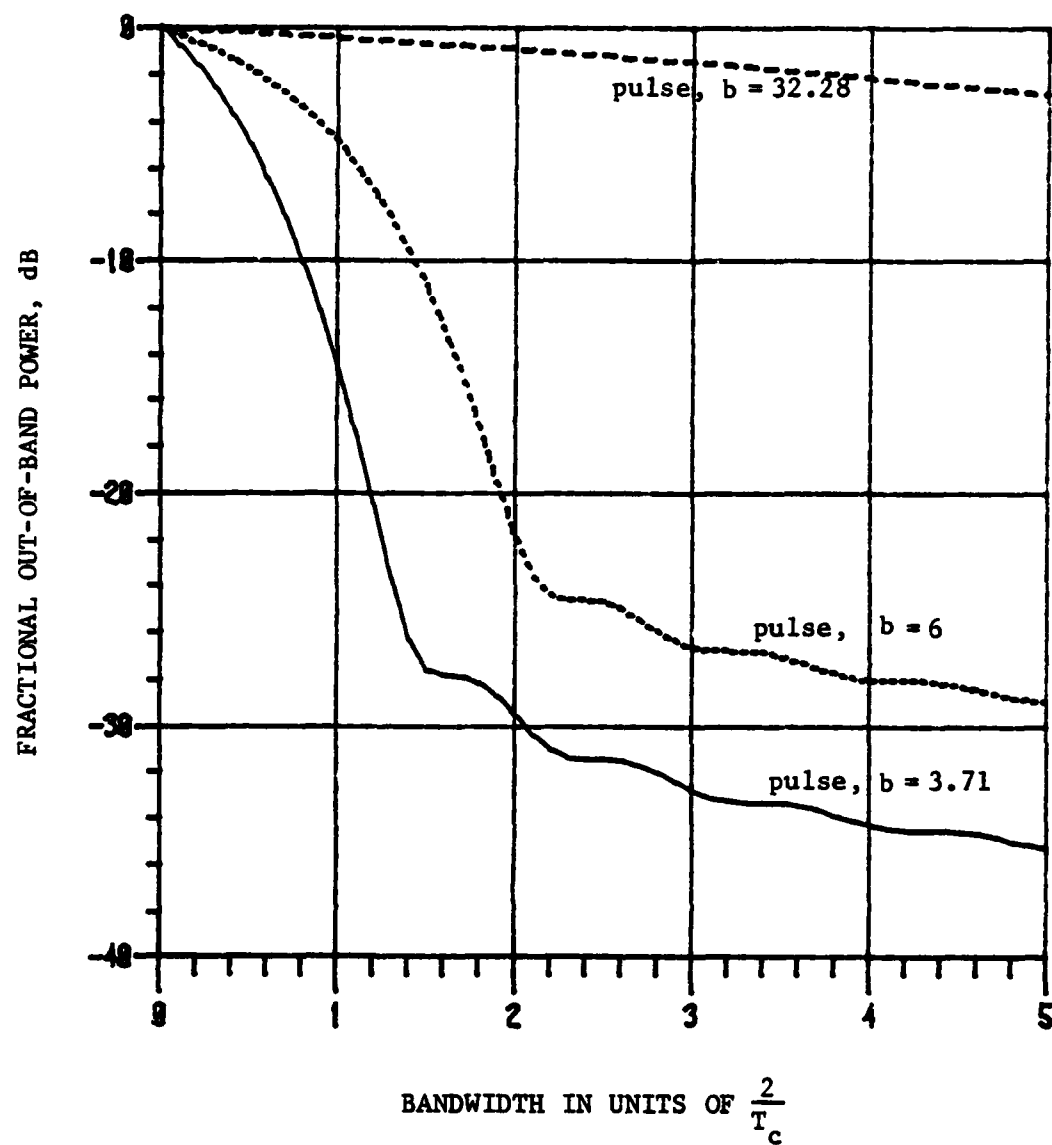


Figure 4.6. Fractional Out-of-Band Power vs. Bandwidth

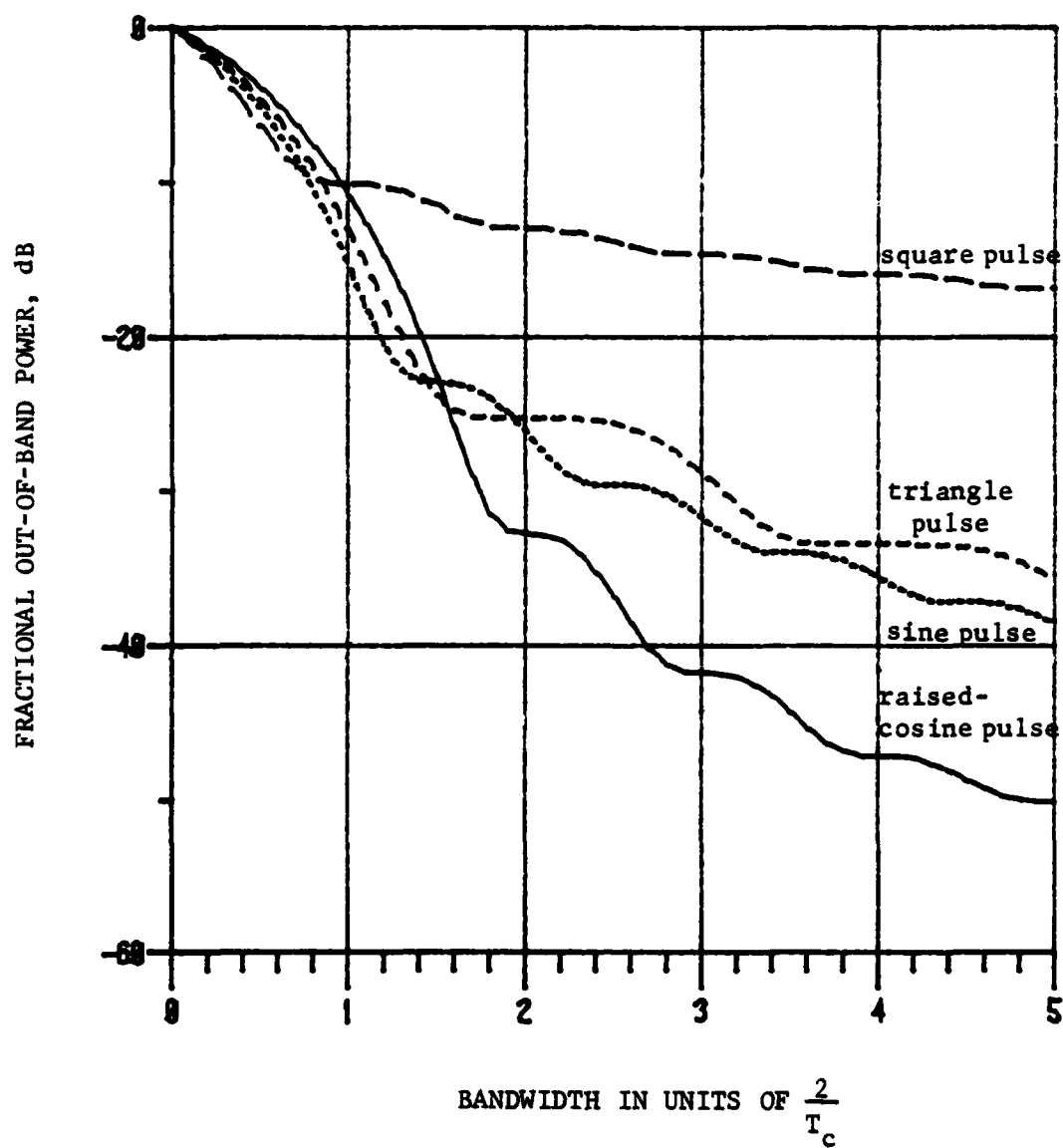


Figure 4.7. Fractional Out-of-Band Power vs. Bandwidth

TABLE 4.1
Chip Waveform Parameters

Chip Waveform	\overline{m}^2	η^2	99% Power Bandwidth in Units of $2/T_c$	Magnitude of Upper Envelope	Magnitude of Lower Envelope
pulse, $b = 3.71$.286	.0376	1.18	1.49	1.33
pulse, $b = 6$.150	.00649	1.92	1.93	.46
pulse, $b = 32.28$.0240	-.000108	10.28	4.58	.23
raised cosine pulse	.241	.00945	1.41	1.63	1.15
sine pulse (MSK)	.293	.0433	1.18	1.41	1.41
triangle pulse	.270	.0268	1.30	1.73	1.22
square pulse (SQPSK)	.333	.167	10.28	1.41	1.41

The following definitions apply:

raised cosine pulse, $\psi(t) = \sqrt{\frac{2}{3}} [1 - \cos(2\pi t/T_c)] P_{T_c}(t)$

sine pulse, $\psi(t) = \sqrt{2} \sin(\pi t/T_c) P_{T_c}(t)$

triangle pulse, $\psi(t) = \sqrt{3} [1 - 2|\frac{t}{T_c} - \frac{1}{2}|] P_{T_c}(t)$

square pulse, $\psi(t) = P_{T_c}(t)$

CHAPTER 5

CONCLUSIONS

We have performed a general analysis of an OQ/DS/SSMA communication system and found the SNR. The expected 99 percent power bandwidths the constant-envelope characteristics of the transmitted signals were found. There exists a complicated interplay between the SNR, the system bandwidth, and the constant-envelope properties of the transmitted signals, but we found methods of choosing a chip waveform for desirable characteristics. We also determined parameters for standard chip waveforms. It was determined that the sine pulse was a good choice for the chip waveform, but that other waveform choices could cause a system parameter to improve, sometimes at the expense of degradation of another desirable parameter.

We should note that the SNR is an important performance index, but that the probability of bit error that results in our system is a main concern. Also our comparisons have been made using the assumption of random binary sequences. The power spectral density of the transmitted signals is one characteristic which will depend somewhat on the actual signature sequences which are chosen, and certainly the SNR will depend on this choice of sequences. Modelling the actual signature sequences by random sequences is reasonable, however, since random sequences are good approximations to long signature sequences. When showing the dependence of the SNR on the chip waveform is through the parameter η^ψ , the effect of the approximation is small since the parameter η^ψ is often much smaller than the parameter $\bar{\eta}^\psi$. Comparisons of different chip waveforms when fixed sequences are chosen verify the validity of the approximations [1].

REFERENCES

1. M. B. Pursley, F. D. Garber, J. S. Lehnert, "Analysis of generalized quadriphase spread-spectrum communications," 1980 IEEE International Conference on Communications, Conference Record, pp. 15.3.1-15.3.6.
2. M. B. Pursley, "Spread spectrum multiple-access communications," in Multi-User Communications, G. Longo (ed.), Springer-Verlag, Vienna, 1980.
3. H. F. A. Roefs, "Binary sequences for spread-spectrum multiple-access communication," Ph.D. Thesis, Department of Electrical Engineering, University of Illinois, (CSL Report No. R-785), August 1977.
4. F. D. Garber and M. B. Pursley, "Performance of offset quadriphase spread-spectrum multiple-access communications," IEEE Transactions on Communications, March 1981 (to appear).
5. M. B. Pursley, unpublished notes, 1979.
6. D. Slepian, "Prolate spheroidal wave functions, Fourier analysis, and uncertainty-IV," Bell System Technical Journal, 43, No. 6 (November 1964), pp. 3009-3058.
7. D. Slepian and H. O. Pollak, "Prolate spheroidal wave functions, Fourier analysis, and uncertainty-I," Bell System Technical Journal, 40, No. 1 (January 1961), pp. 43-64.
8. H. J. Landau and H. O. Pollak, "Prolate spheroidal wave functions, Fourier analysis, and uncertainty-II," Bell System Technical Journal, 40, No. 1 (January 1961), pp. 65-84.
9. H. J. Landau and H. O. Pollak, "Prolate spheroidal wave functions, Fourier analysis and uncertainty-III," Bell System Technical Journal, 41, No. 4 (July 1962), pp. 1295-1336.
10. D. Slepian, "On bandwidth," Proceedings of the IEEE, 64, No. 3 (March 1976), pp. 292-300.
11. M. B. Pursley, "Performance evaluation for phase-coded spread-spectrum multiple-access communication -- Part I: System analysis," IEEE Transactions on Communications, vol. COM-25, August 1977, pp. 795-799.
12. M. B. Pursley and D. V. Sarwate, "Performance evaluation for phase-coded spread-spectrum multiple-access communication -- Part II: Code sequence analysis," IEEE Transactions on Communications, vol. COM-25, August 1977, pp. 800-803.

END

FILMED